Accepted Manuscript

Effect of ultrasound on physicochemical properties of emulsion stabilized by fish myofibrillar protein and xanthan gum

Yao Xiong, Qianru Li, Song Miao, Yi Zhang, Baodong Zheng, Longtao Zhang

PII: S1466-8564(18)31227-X
DOI: https://doi.org/10.1016/j.ifset.2019.04.013
Reference: INNFOO 2160

To appear in: *Innovative Food Science and Emerging Technologies*

Received date: 6 October 2018
Revised date: 3 January 2019
Accepted date: 29 April 2019

Please cite this article as: Y. Xiong, Q. Li, S. Miao, et al., Effect of ultrasound on physicochemical properties of emulsion stabilized by fish myofibrillar protein and xanthan gum, Innovative Food Science and Emerging Technologies, https://doi.org/10.1016/j.ifset.2019.04.013

Effect of ultrasound on physicochemical properties of emulsion stabilized by fish myofibrillar protein and xanthan gum

Yao Xiong [a, b, c], Qianru Li [a, b, c], Song Miao *[d, b], Yi Zhang [a, b, c], Baodong Zheng [a, b, c], Longtao Zhang *[a,b,c]

[a] *College of Food Science, Fujian Agriculture and Forestry University, Fuzhou 350002, P. R. China*

[b] *China-Ireland International Cooperation Centre for Food Material Science and Structural Design, Fujian Agriculture and Forestry University, Fuzhou, Fujian*

[c] *Fujian Provincial Key Laboratory of Quality Science and Processing Technology in Special Starch, Fujian Agriculture and Forestry University, Fuzhou 350002, P. R. China*

[d] *Teagasc Food Research Centre, Moorepark, Fermoy, Co. Cork, Ireland*

* Corresponding authors:

Song Miao, E-mail: song.miao@teagasc.ie

Longtao Zhang, E-mail: zlongtao@fafu.edu.cn

Abstract

To investigate the effects ultrasound (20 kHz, 150–600 W) on physicochemical properties of emulsion stabilized by myofibrillar protein (MP) and xanthan gum (XG), the emulsions were characterized by Fourier transform infrared (FT-IR) spectroscopy, ζ-potential, particle size, rheology, surface tension, and confocal laser scanning microscopy (CLSM). FT-IR spectra confirmed the complexation of MP and XG, and ultrasound did not change the functional groups in the complexes. The emulsion treated at 300 W showed the best stability, with the lowest particle size, the lowest surface tension (26.7 mNm^{-1}) and the largest ζ-potential absolute value (25.4 mV), that were confirmed in the CLSM photos. Ultrasound reduced the apparent viscosity of the MP-XG emulsions, and the changes of particle size were manifested in flow properties. Generally, ultrasound was successfully applied to improve the physical stability of MP-XG emulsion, which could be used as a novel delivery system for functional material.

Keywords: ultrasound; myofibrillar protein; emulsion; stability; xanthan gum

1. Introduction

Myofibrillar proteins (MPs), the main component of fish meat, are amphiphilic molecules with the best emulsifying properties available in meat systems (Sarma, Reddy, & Srikar, 2000*)*, and can be used as emulsifiers (Jiang & Xiong, 2015; Lam & Nickerson, 2013). While, MP emulsions are generally prone to aggregation and flocculation. It is necessary to investigate the available ingredients and methods to improve the physical stability of MP emulsions.

Proteins and polysaccharides often co-exist in food emulsion systems, and can form complexes under different conditions (Van, De, Oosterveld, & Tromp, 2015). The strength of the interactions between proteins and polysaccharides at the interface is related to the stability, aggregation, flocculation, and delamination of the emulsion. Ganzevles et al. (2007) investigated the effect of different ratios of pectin and β-lactoglobulin on the structure of the interfacial adsorption layer, and found that the complex formed a denser interfacial film under neutral conditions. Sato et al. (2003) demonstrated that the addition of alginic oligosaccharides can improve the emulsifying ability and emulsion stability of water-soluble MPs. Lu et al. (2018) reported an O/W emulsion with better stability and controlled release of β-carotene by constructing a water phase with the functional konjac glucomannan. Generally, soluble complexes formed by electrostatic interactions between protein and polysaccharide can create a protective layer at the oil–water interface, which is beneficial to the improvement of emulsion stability (Thepkunya, Rungnaphar, & Mcclements, 2006). Xanthan gum (XG) is an anionic polysaccharide with good stability in terms of temperature, pH, salts, and enzyme degradation. It is usually

added in the aqueous phase to improve the stability of the oil-in-water (O/W) emulsion. Thus far, no studies on the stability of MP emulsions with XG have been reported. In the present study, we examined the preparation of stable O/W emulsions using MP and XG, both of which are surfactants.

Ultrasound can enhance the functional properties of biopolymers, producing stable emulsions with little requirement for surfactants (Kaltsa, Michon, Yanniotis, & Mandala, 2013). Albano and Nicoletti (2018) successfully improved the stability of a whey protein concentrate–pectin emulsion using ultrasound. Similarly, Sui et al. (2017) demonstrated that the emulsifying activity index and emulsion stability index of an emulsion system stabilized with soybean protein isolate and lecithin increased after ultrasound treatment. Little is known about the application of ultrasound processes on fish protein-based emulsion products, which have different structure than plant protein or Pork/chicken protein which could lead to form different emulsion delivery system. To date, there have been no reports on the ultrasound treatment of MP-XG emulsion.

Thus, the purpose of this study was to investigate the effects of 20-kHz ultrasound at varying power (150–600 W) on the stability of MP-XG emulsions. The effect of ultrasound treatments on functional groups, microstructure, and rheological properties of the samples was also evaluated.

2. Materials and methods

2.1 Materials

Nemipterus virgatus surimi was provided by Haixin Foods Co., Ltd. (Fujian, China). Xanthan gum (USP, PubChem CID: 7107) was purchased from Aladdin

Industrial Co., Ltd. (Shanghai, China). Commercial soybean oil was obtained from a local supermarket. The stain Nile blue was purchased from Alfa Aesar Chemical Co., Ltd. (Shanghai, China), and Nile red was purchased from Acros Organics (Shanghai, China). All other chemical reagents were of analytical grade. Deionized water was used for preparing and diluting the solutions.

2.2 Mixture preparation

Thawed *Nemipterus virgatus* surimi was homogenized in four volumes of isolation buffer (10 mM sodium phosphate, 0.1 M NaCl, 2 mM $MgCl_2$, 1 mM EGTA, pH 7.0) for 60 s with a PRO-12S blender (German Pool Ltd., Hong Kong, China) at maximum speed. The suspension was centrifuged at 3000 *g* for 15 min at 4 °C (Avanti J-E; Beckman Coulter, Brea, CA, USA). The pellet was collected and resuspended in four volumes of the same phosphate buffer. After three repeated cycles of homogenization and centrifugation, the resulting pellet was mixed with four volumes of washing solution (0.1 M NaCl), further homogenized, and centrifuged under the same conditions. This step was repeated twice. The final pellet was resuspended and homogenized in four volumes of the same washing solution, and then adjusted to pH 6.25 with 0.1 N HCl prior to centrifugation. The purified MP pellet was stored on ice and utilized within 48 h of isolation. Protein concentration was measured by the Biuret method (Gornall, Bardawill, & David, 1949), with bovine serum albumin as the standard.

The MP was dissolved and adjusted to a concentration in a dilute buffer solution (50 mM sodium phosphate, 0.6 M NaCl, pH 6.25). The MP solution was stored at 4 °C overnight to ensure sufficient hydration. A certain amount of XG was dissolved in the same dilution buffer solution, and the adjusted MP solution was then added and stirred for 4 hours.

2.3 Ultrasound treatment

A 100-mL aliquot of the MP-XG mixture was transferred to a jacketed beaker (250 mL) with circulating cooled water. The mixtures were treated at 20 kHz at different levels of power output (0 W, 150 W, 300 W, 450 W, 600 W) for 12 min (pulse duration of on-time 4 s and off-time 2 s) using a Scientz-950E ultrasound generator (Scientz Biotechnology Co., Ltd, Ningbo, China) with a12 mm vibrating titanium tip probe. A 5-mL aliquot of the treated MP-XG mixture was taken out and freeze-dried.

2.4 Preparation of O/W emulsions

The MP-XG emulsion system was prepared according to the method of Wu et al. (2009) with slight modifications. A solution containing 90% (v/v) ultrasonicated MP-XG mixture and 10% (v/v) soybean oil was emulsified at 18,000 rpm for 2 min using an Ultra Turrax homogenizer (T18 Basic; IKA, Staufen, Germany). The MP-XG-stabilized O/W emulsions with 0.9% (w/v) MP and 0.3% (w/v) XG were prepared by homogenization, and the mass ratio of MP and XG in the final emulsion was always maintained at 3:1. The pH were adjusted to 7.0 using 0.1 M NaOH. Fresh emulsion (5.0 mL) samples were transferred into glass test tubes (internal diameter, 1.6 cm; height, 3 cm) and tightly sealed with a black plastic cap to prevent evaporation.

2.5 FT-IR spectroscopy

A Vertex 70 series Fourier-transform infrared (FT-IR) spectrometer (Bruker Optics Co., Ettlingen, Germany) was used for the FT-IR spectroscopy analysis. Pure MP, XG, and the MP-XG ultrasound-treated at different power levels were mixed with dried KBr at a ratio of 1:10, and then grounded and pressed into a pellet, respectively. Spectra were obtained at a resolution of 4 cm^{-1} in the range of 4000–400 cm^{-1}, and

were averaged over 32 scans (Carpenter & Saharan., 2017). All spectra were baseline corrected using PeakFit 4.12 (SeaSolve Software Inc., San Jose, CA, USA) after deducting the background.

2.6 Surface tensiometry

A BZY series automatic surface tension meter (Shanghai HengPing Instrument and Meter Factory, China) with a platinum Wilhelmy plate was used to measure the surface tension of the samples (Fu et al., 2018). MP-XG emulsions prepared under different ultrasonic conditions were transferred into the measuring vessel, respectively. The surface tension (mNm^{-1}) was measured at room temperature, with at least three parallel measurements made for each group of samples.

2.7 Rheological properties

Rheological measurements were carried out using a physica MCR 301 rotational rheometer (Anton Paar GmbH, Graz, Austria) equipped with PP 50 (1-mm gap) parallel plate geometry, according to the method of Osano et al. (2014) with some modifications. Each sample was equilibrated for 60 s before testing.

Apparent viscosity was determined over a shear rate range of 0.01–100 s^{-1} at 25 ± 1 °C and fitted to a power-law model (Ostwald–de Waele model) as follows:

$$\tau = K \cdot \gamma^{n}$$

where τ is the viscosity (Pa·s); γ is the shear rate (s^{-1}); K is the consistency index ($Pa \cdot s^{n}$); and n is the flow behavior index.

A dynamic frequency sweep was applied, with a constant stress of 0.5% over a frequency range of 0.01–10 Hz. The storage modulus (G') and loss modulus (G") were recorded.

2.8 Particle size distribution

A Mastersizer 3000 Laser particle size analyzer (Malvern Instruments, Malvern,

UK) was used to determine the mean particle diameter and droplet size distribution of the emulsions (Tsabet & Fradette., 2015). The samples were diluted ten times using deionized water of the appropriate pH to avoid multiple light scattering (Mcclements, Decker, & Choi, 2014). For the test, the laser obscuration level was set at 10%, and the parameters of refractive index were set to 1.520 for the emulsion particles and 1.330 for the deionized water. The samples were equilibrated for 90 s inside the instrument before the data were collected, with at least 12 sequential readings obtained.

2.9 ζ-Potential

A Zetasizer Nano ZS90 potential analyzer (Malvern Instruments, Malvern, UK) was used to evaluate the droplet charge of the emulsions (Kong et al., 2017). MP-XG complexes that had undergone different treatments were diluted with a same buffer solution, and the diluted complexes were then filtered through a 0.45-μm filter and used for the ζ-potential determination. Samples were equilibrated for 120 s inside the instrument before the data were collected, with at least 12 sequential readings.

2.10 Confocal laser scanning microscopy

A Leica TCS SP8® microscope (Leica Microsystems GmbH, Wetzlar, Germany) with a 40× (NA 1.25) oil immersion objective lens was used to observe the microstructure of the samples. The CLSM was operated in the fluorescence mode. Nile blue was used to stain the dispersed phase, and Nile red was used to stain the oil phase. All of the stain solutions were prepared at room temperature and stored in a dark place. Approximately 0.5 mL of the samples were completely mixed with a 20-μL aliquot of the Nile blue (0.01%, w/v) and Nile red (0.01%, w/v) solutions. Approximately 80 μL of the stained samples was immediately placed into a laboratory-made welled slide (Moschakis, Murray, & Dickinson, 2005) and carefully

covered with a coverslip, ensuring that there was no trapped air gap or bubbles between the mixture and the cover slip. The mixtures were equilibrated for 2 min before observation. The images were collected using 488- and 633-nm excitation wavelengths for Nile blue and Nile red, respectively. Each image contained 1024 × 1024 pixels.

2.11 Physical stability

A multisample analytical centrifuge (LUMiFuge; LUM GmbH, Berlin, Germany) was used to evaluate the physical stability of the samples. Samples (420 μL) were transferred to polycarbonate rectangular cells (2 × 8 mm) and analyzed by a light beam emitted at a near-infrared wavelength (880 nm) that scanned the sample cells over the total length (Mao, Roos, & Miao, 2015). The particle movement rate is related to the stability of the emulsion. Therefore, the lower the creaming rate, the higher the stability. In the present study, the samples in the LUMiFuge were centrifuged at 286.8 *g* and 25 °C, with a scanning rate of once every 30 s for 2.1 h.

2.12 Statistical analysis

All experiments were repeated at least twice using the same freshly prepared emulsion. Data analysis was performed using OriginPro 8.5 (Northampton, MA, USA). One-way analysis of variance using the Tukey procedure was applied to determine the significance ($p < 0.05$) of the differences between means.

3. Results and discussion

3.1 FT-IR spectroscopy

Fig. 1a showed the FT-IR spectra of MP, XG, and the MP-XG without ultrasound treatment. The pure MP spectrum has a broad and strong absorption band at 3423 cm^{-1} related to O-H stretching vibration. The absorption band at 2924 cm^{-1} was caused by C-H stretching vibration, and that at 1651 cm^{-1} by C=O stretching vibration.

The presence of the peak at 1542 cm^{-1} can be attributed to the in-plane bending vibration of N-H, and the weak absorption band at 1157 cm^{-1} was associated with C-N stretching vibration. Similar observations of MP absorbance spectra have been reported (Liu et al., 2017).

The pure XG spectrum revealed characteristic functional groups (Fig. 1a): the broad band at 3429 cm^{-1} refers to the stretching vibration of O-H; the band at 2924 cm^{-1} was caused by the stretching vibration of C-H; the absorption band at 1736 cm^{-1} represents the stretching vibration of C=O; the bands at 1637 $cm^{-1}$and 1420 cm^{-1} were caused by the asymmetric and symmetric vibrations of -COO-, respectively; and finally, the band at 1051 cm^{-1} corresponds to the stretching vibration of C-O-C. Our results were consistent with those of Babaladimath and Chapi (2018).

For the untreated MP-XG sample, the strong absorption bands at 2924 and 2855 cm^{-1} represent the asymmetric and symmetric stretching vibrations of $-CH_2$, respectively. Unlike XG, no characteristic absorption peaks were observed at 1736 and 1420 cm^{-1} of the MP-XG. This result may be due to the electrostatic interactions between the positively charged amino groups in MP and the negatively charged carboxylic acid groups in XG, resulting in the formation of an amine-containing complex.

The infrared spectra of the MP-XG treated under different ultrasonic conditions were shown in Fig. 1b. No significant changes were observed in the treated MP-XG mixtures compared to the untreated sample, which showed that the functional groups of the MP-XG remained unchanged after ultrasound treatment. Another study on the effect of ultrasound on O/W emulsions of whey protein concentrate–pectin complexes reached similar conclusions (Albano, et al., 2018).

3.2 Surface tension analysis

Surface tension is one of the most important properties of emulsions, and it directly affects the physical and chemical properties of the emulsion interfacial film (W. Jiang, et al., 2005). Table 1 showed that the surface tension of the untreated emulsion was 34.8 mNm^{-1}, whereas that of the ultrasound-treated emulsions was significantly lower ($p < 0.05$). The lowest surface tension was 26.7 mNm^{-1} in the 300 W sample. It was inferred that ultrasound can speed up the migration of protein molecules at the oil–water interface, thereby reducing the surface tension of the proteins (Arzeni, Pérez, & Amr, 2012; Hu, et al., 2013). When the ultrasonic power reached 600 W, the MP-XG complex tended to self-aggregate, leading to decreased stretching adsorption at the oil–water interface. Cheng et al. (2011) demonstrated that moderate sonication can significantly increase the emulsifying capacity of protein–polysaccharide complexes and improve their ability to reduce the thermodynamic instability of the interface.

3.3 Analysis of rheological properties

The shear force generated by ultrasonic cavitation can change the degree of aggregation of the protein molecules in the solution, which in turn affects the rheological properties of the protein solution. Emulsion fluidity is generally characterized by apparent viscosity (Choe, Kim, Lee, Kim, & Kim, 2013). The effect of different levels of ultrasound on the apparent viscosity of the emulsion samples in the shear rate range from 0.01 to 100 s^{-1} was shown in Fig. 2. Table 1 listed the corresponding fitting parameters of the power-law model. All of the MP-XG emulsions conformed to the Ostwald–de Waele model and exhibited shear thinning behavior ($n < 1$), which indicated that the viscosity decreased with increasing shear rate. As the ultrasonic power increased, the initial viscosity of the emulsion ranged from 4.38 $mPa \cdot s^{-1}$ (150 W) to 0.146 $mPa \cdot s^{-1}$ (600 W), which was significantly ($p <$

0.05) lower than that of the untreated group. Ultrasound apparently reduced the value of K and increased the value of n, and this can be attributed to the ultrasonic cavitation effect, which destroyed the hydrophobic interactions between the protein molecules and changed the rheological properties of the samples. Similar conclusions have been reported previously (Chandrapala, Zisu, Palmer, Kentish, & Ashokkumar, 2011). However, the findings of Krešić et al. (2008) are contrary to ours. The reason for this difference may be that there was no temperature control during sonication in their experiments, and the ultrasound treatment changed the structure of the protein molecules, causing the protein to polymerize.

The oscillation test was used to assess the relationship between the internal structure and the macroscopic rheology, and this test allowed a comprehensive analysis of the rheological properties of the emulsion. Fig. 3 showed the effect of different ultrasound treatment on the G' and G" of the emulsions. The results exhibited that the G' of the emulsions was greater than G" in the measured frequency range (Fig. 3a and b), which could potentially be attributed to the weak gel structure of the emulsions. Results for the untreated emulsion showed that the G' slightly but progressively increased with increasing oscillation frequency in the range of linear viscoelasticity, implying that the strong interactions mainly contributing to the elastic modulus needed a long time to relax (Manoi & Rizvi, 2009). This phenomenon indicated that emulsion still possessed permanent interactions which gave a predominantly solid behavior at low frequency (Niu, et al., 2016). However, results for the ultrasonic-treated emulsion showed that the G' increased with the rise of frequency, and they were almost frequency dependent. In addition, the ultrasound treatment reduced the G' and G" of the emulsion compared to the untreated emulsion, which was a similar result to that found in a study on the effect of high-intensity

sonication on soy protein isolates (Hu, et al., 2013). Thus, it was possible that the changes in the particle size distribution (Section of particle size distribution) of the treated emulsions were manifested in the flow properties (Arzeni, et al., 2012). The above results suggest that ultrasound treatment changed the rheological properties of the MP-XG emulsions.

3.4 Particle size distribution

Emulsion stability can be characterized by droplet size and distribution, wherein the surface-weighted mean size (d_{32}) is sensitive to the presence of small particles in the emulsion, as reflected in the emulsifying properties of the food emulsion (Chen, Chen, Ren, & Zhao, 2011); the volume-weighted mean size (d_{43}) is sensitive to the presence of large particles in the emulsion, as shown by the aggregation or flocculation of the food emulsion (Lesmes & Mcclements, 2009). Fig. 4 showed the particle size distribution of the freshly prepared emulsions and the macroscopic morphology after storage for 20 days. The corresponding particle sizes, d_{43} and d_{32}, were shown in Table 1. Compared to the untreated emulsion, the ultrasonic-treated emulsions demonstrated better stability with smaller particle size. A possible reason for this result could be that the shear force generated by the cavitation of the ultrasonic waves led to a decrease in the particle size of the emulsion. The emulsion treated at 600 W exhibited a wider particle size distribution, indicating inconsistent size and uneven size distribution of the droplet particles. The macroscopic image of the sample stored for 20 days also showed storage instability. Sui, Bi, Qi, Wang, Zhang, Li, and Jiang (2017) reported that high-intensity sonication resulted in the simultaneous occurrence of fragmentation and agglomeration of the particles, which was also reflected in our rheology results.

The d_{43} and d_{32} values of the treated samples were significantly lower ($p < 0.05$)

than those of the untreated emulsion (the d_{43} value decreased from 18.4 μm to 12.0 μm, and the d_{32} value decreased from 10.4 μm to 6.5 μm), indicating that the sonicated samples had better emulsification properties. Yanjun et al. (2014) treated a milk protein concentrate solution at an ultrasonic intensity of 12.5 W, and successfully reduced the mean particle size (d_{50}) of the solution. However, the 600-W-treated emulsion showed larger d_{43} and d_{32} values, suggesting a certain degree of aggregation.

3.5 ζ-Potential analysis

Based on the mechanism of dynamic light scattering, the electrophoretic migration rate of the particles can be evaluated indirectly by measuring the frequency or phase change of light. The surface charge of the emulsion is affected by the electrostatic interactions between the protein and the polysaccharide (Wagoner, Vardhanabhuti, & Foegeding, 2016). In general, the greater the absolute value of the ζ-potential, the stronger the electrostatic repulsive force and the more stable the emulsion (Dickinson, 2009).

The potential changes of the MP-XG O/W emulsions sonicated at different power levels were shown in Fig. 5. The ζ-potential of the untreated MP-XG emulsion was approximately –18.4 mV. When the ultrasonic power was less than 450 W, the absolute value of the ζ-potential of the ultrasonic-treated emulsion was significantly higher ($p < 0.05$) than that of the untreated emulsion. With increasing ultrasonic power, the potential change between the emulsions in each group showed a trend of firstly increasing and then decreasing. The 300-W-treated emulsion had the largest ζ-potential absolute value of 25.4 mV, which implied that relatively low ultrasound intensity opened up the internal structure of the myofibrillar molecules and increases their contact with XG. Shanmugam and Ashokkumar (2014) used ultrasound to prepare a stable flaxseed oil emulsion. They found that ultrasound promoted the

electrostatic interactions between the protein and the polysaccharide, thus promoting protein alignment, which bolstered the stability of the system. However, ultrasound above 300 W caused the protein to aggregate and shielded some of the charged groups, reflecting the weak interactions between MP and XG.

3.6 Emulsion microstructure

CLSM was used to observe the interface composition of the emulsion and the adsorption of the emulsifiers at the oil–water interface. The micrograph indicated droplet aggregation and flocculation of the emulsions. The oil phase was stained green by Nile red, and the aqueous phase was stained red by Nile blue. Orange showed the mixing of the proteins and lipids.

As seen in Fig. 6a, the untreated group had a larger mean oil droplet size and non-uniform particle size; further, local aggregation occurred, indicating low stability. With increasing ultrasonic power, the droplet size first decreased and then increased. The lowest emulsion particle size was observed for the 300-W-treated emulsion (Fig. 6c), which was consistent with the particle size measurement. The droplets with the larger particle sizes showed a dense distribution at 450 W; however, no obvious aggregation was observed (Fig. 6d). For the emulsion treated at 600 W, red fluorescence not only appeared clearly on the surface of the oil droplet, but was also observed inside the solution (Fig. 6e). This finding suggests that the protein molecules not only adsorbed on the surface of the droplets but also exhibited self-aggregation at an ultrasonic power level of 600 W. It can be inferred that insoluble aggregates were formed. Jiang et al. (2014) investigated the effect of different levels of ultrasonic power and ultrasound time on the structure and function of black bean protein isolate (BBPI). The results showed that sonication accelerated and destroyed the molecular motion of BBPI, causing protein aggregation. In conclusion, excessive sonication

results in changes in the molecular structure of the protein and reduced its emulsifiability. The lack of emulsifier adsorbed on the surface of the oil droplets made the emulsion droplets larger, leading to an unstable emulsion.

3.7 Physical stability analysis

Fig. 7 showed the analysis of the tested emulsions using LUMiFuge stability analyzer, as well as the macro photograph of the sample after centrifugation. The first scanning profile obtained is marked in red at the bottom, and the last in green at the top. The obtained spectrum recorded the migration of particles in the emulsion, and can be used to estimate the stability of the emulsion during storage (Sobisch & Lerche, 2008). The greater the change in light transmittance during the acceleration of the emulsion, the worse the stability (Yuan, Xu, Qi, Zhao, & Gao, 2013).

The untreated emulsion maintained a low light transmission rate after centrifugation at 1500 rpm for 2.1 h (Fig. 7a). A stable interfacial layer was formed on the surface of the oil droplet through electrostatic interactions between MP and XG; however, the particle size results and the CLSM photos showed that the droplet size was large. The changes in the transmission of the treated emulsions at 150 W and 300 W were similar to those in the untreated emulsion (Fig. 7b and c), suggesting that emulsions under these conditions have a relatively long shelf life. The transmittance of the emulsion formed by ultrasound at 450 W increased with increasing centrifugation time (Fig. 7d), reflecting the uneven distribution of the particles and the accumulation of the particles caused by their upward migration during storage. For the emulsion treated at 600 W (Fig. 7e), the light transmittance increased rapidly during the initial period of centrifugal acceleration. The obvious phase separation could also be seen in the macro sample pictures, which indicated the worst storage stability in this sample. Combined with the surface tension, particle size, ζ-potential,

and CLSM data, these results suggested that the 300-W-treated emulsion had the most uniform droplet distribution and best storage stability of all the samples.

4. Conclusion

In this work, MP-XG complexes were formed and play an important role as an emulsifier in the emulsion preparation and were not changed by ultrasound. Ultrasonic power of 300 W reduced the particle size and surface tension of the emulsion, and increased its storage stability. Ultrasound reduced the apparent viscosity of the MP-XG emulsions, and the changes of particle size were manifested in flow properties. The results demonstrated that ultrasound can effectively improve the stability of MP-XG emulsions, which can be useful in the rational design of MP-based emulsion delivery systems with better functional properties.

Acknowledgments

This work supported by International Science and Technology Cooperation and Exchange Program of Fujian Agriculture and Forestry University (KXGH17001), Fujian Provincial Foreign Cooperation Project (2018I0003), Fujian Provincial Science and Technology Program of Regional Development Project (2018N3001) and National Natural Science Foundation of China (31628016).

References

Albano, K. M., & Nicoletti, V. R. (2018). Ultrasound impact on whey protein concentrate-pectin complexes and in the O/W emulsions with low oil soybean content stabilization. *Ultrasonics Sonochemistry,* 41, 562–571.

Arzeni, C., Pérez, O. E., & Amr, P. (2012). Functionality of egg white proteins as affected by high intensity ultrasound. *Food Hydrocolloids, 29*(2), 308-316.

Babaladimath, G., & Chapi, S. (2018). Microwave-assisted synthesis, characterization of electrical conducting and electrochemical xanthan gum-graft-polyaniline. *Journal of Materials Science Materials in Electronics*, 1-8.

Carpenter, J., & Saharan, V. K. (2017). Ultrasonic assisted formation and stability of mustard oil in water nanoemulsion: Effect of process parameters and their optimization. *Ultrasonics Sonochemistry, 35*(Part A), 422-430.

Chandrapala, J., Zisu, B., Palmer, M., Kentish, S., & Ashokkumar, M. (2011). Effects of ultrasound on the thermal and structural characteristics of proteins in reconstituted whey protein concentrate. *Ultrasonics Sonochemistry, 18*(5), 951-957.

Chen, L., Chen, J., Ren, J., & Zhao, M. (2011). Modifications of soy protein isolates using combined extrusion pre-treatment and controlled enzymatic hydrolysis for improved emulsifying properties. *Food Hydrocolloids, 25*(5), 887-897.

Cheng, Q., Decker, E. A., Hang, X., & Mcclements, D. J. (2011). Comparison of Biopolymer Emulsifier Performance in Formation and Stabilization of Orange Oil-in-Water Emulsions. *Journal of the American Oil Chemists Society, 88*(1), 47-55.

Choe, J. H., Kim, H. Y., Lee, J. M., Kim, Y. J., & Kim, C. J. (2013). Quality of frankfurter-type

sausages with added pig skin and wheat fiber mixture as fat replacers. *Meat Science, 93*(4), 849-854.

Dickinson, E. (2009). Hydrocolloids as emulsifiers and emulsion stabilizers. *Food Hydrocolloids, 23*(6), 1473-1482.

Fu, D., Xie, J., Wang, F., & Wang, S. (2018). Investigation of surface tension and viscosity for aqueous solutions of MEA-MeOH and DEA-MeOH. *Journal of Chemical Thermodynamics, 116*, 197-205.

Ganzevles, R. A., Vliet, T. V., Stuart, M. A. C., & Jongh, H. H. J. D. (2007). Manipulation of Adsorption Behaviour at Liquid Interfaces by Changing Protein-Polysaccharide Electrostatic Interactions. In *Conference on Food Colloids, 21*,195-208.

Gornall, A. G., Bardawill, C. J., & David, M. M. (1949). Determination of serum proteins by means of the biuret reaction. *Journal of Biological Chemistry, 177*(2), 751-766.

Hu, H., Wu, J., Li-Chan, E. C. Y., Zhu, L., Zhang, F., Xu, X., Fan, G., Wang, L., Huang, X., & Pan, S. (2013). Effects of ultrasound on structural and physical properties of soy protein isolate (SPI) dispersions. *Food Hydrocolloids, 30*(2), 647-655.

Jiang, J., & Xiong, Y. L. (2015). Role of interfacial protein membrane in oxidative stability of vegetable oil substitution emulsions applicable to nutritionally modified sausage. *Meat Science, 109*, 56-65.

Jiang, L., Wang, J., Li, Y., Wang, Z., Liang, J., Wang, R., Chen , Y., Ma, W., Qi, B., & Zhang, M. (2014). Effects of ultrasound on the structure and physical properties of black bean protein isolates. *Food Research International, 62*(6), 595-601.

Jiang, W., Chen, Z., Liu, Y., Zou, H., Li, J., Wang, H., & Jiang, W. (2005). Computer Simulation of

Surface Tension for Complex Emulsion System. *Journal of Mathematical Chemistry, 38*(4), 685-693.

Kaltsa, O., Michon, C., Yanniotis, S., & Mandala, I. (2013). Ultrasonic energy input influence on the production of sub-micron o/w emulsions containing whey protein and common stabilizers. *Ultrasonics Sonochemistry, 20*(3), 881-891.

Kong, X., Jia, C., Zhang, C., Hua, Y., & Chen, Y. (2017). Characteristics of soy protein isolate/gum arabic-stabilized oil-in-water emulsions: influence of different preparation routes and pH. *Rsc Advances, 7*(51), 31875-31885.

Krešić, G., Lelas, V., Jambrak, A. R., Herceg, Z., & Brnčić, S. R. (2008). Influence of novel food processing technologies on the rheological and thermophysical properties of whey proteins. *Journal of Food Engineering, 87*(1), 64-73.

Lam, R. S. H., & Nickerson, M. T. (2013). Food proteins: A review on their emulsifying properties using a structure–function approach. *Food Chemistry, 141*(2), 975-984.

Lesmes, U., & Mcclements, D. J. (2009). Structure-function relationships to guide rational design and fabrication of particulate food delivery systems. *Trends Food Sci Tech, 25*, 448–457.

Liu, S., Zhao, P., Zhang, J., Xu, Q., Ding, Y., & Liu, J. (2017). Physicochemical and functional properties of silver carp (Hypophthalmichthys molitrix) myofibrillar protein glycated with konjac oligo-glucomannan. *Food Hydrocolloids, 67*, 216-223.

Lu, W., Zheng, B., & Miao, S. (2018). Improved emulsion stability and modified nutrient release by structuring O/W emulsions using konjac glucomannan. *Food Hydrocolloids, 81*, 120-128.

Manoi, K., & Rizvi, S. S. H. (2009). Emulsification mechanisms and characterizations of cold, gel-like emulsions produced from texturized whey protein concentrate. *Food Hydrocolloids, 23*(7),

1837-1847.

Mao, L., Roos, Y. H., & Miao, S. (2015). Effect of maltodextrins on the stability and release of volatile compounds of oil-in-water emulsions subjected to freeze–thaw treatment. *Food Hydrocolloids, 50*, 219-227.

Mcclements, D. J., Decker, E. A., & Choi, S. J. (2014). Impact of Environmental Stresses on Orange Oil-in-Water Emulsions Stabilized by Sucrose Monopalmitate and Lysolecithin. *J Agric Food Chem, 62*(14), 3257-3261.

Moschakis, T., Murray, B. S., & Dickinson, E. (2005). Microstructural evolution of viscoelastic emulsions stabilised by sodium caseinate and xanthan gum. *Journal of Colloid & Interface Science, 284*(2), 714-728.

Niu, F., Niu, D., Zhang, H., Chang, C., Gu, L., Su, Y., & Yang, Y. (2016). Ovalbumin/gum arabic-stabilized emulsion: Rheology, emulsion characteristics, and Raman spectroscopic study. *Food Hydrocolloids, 52*, 607-614.

Osano, J. P., Hosseini-Parvar, S. H., Matia-Merino, L., & Golding, M. (2014). Emulsifying properties of a novel polysaccharide extracted from basil seed (Ocimum bacilicum L.): Effect of polysaccharide and protein content. *Food Hydrocolloids, 37*, 40-48.

Sarma, J., Reddy, G. V. S., & Srikar, L. N. (2000). Effect of frozen storage on lipids and functional properties of proteins of dressed Indian oil sardine (Sardinella longiceps). *Food Research International, 33*(10), 815-820.

Sato, R., Katayama, S., Sawabe, T., & Saeki, H. (2003). Stability and emulsion-forming ability of water-soluble fish myofibrillar protein prepared by conjugation with alginate oligosaccharide. *J Agric Food Chem, 51*(15), 4376-4381.

Shanmugam, A., & Ashokkumar, M. (2014). Ultrasonic preparation of stable flax seed oil emulsions in dairy systems – Physicochemical characterization. *Food Hydrocolloids, 39*(2), 151-162.

Sobisch, T., & Lerche, D. (2008). Thickener performance traced by multisample analytical centrifugation. *Colloids & Surfaces A Physicochemical & Engineering Aspects, 331*(1–2), 114-118.

Sui, X., Bi, S., Qi, B., Wang, Z., Zhang, M., Li, Y., & Jiang, L. (2017). Impact of ultrasonic treatment on an emulsion system stabilized with soybean protein isolate and lecithin: Its emulsifying property and emulsion stability. *Food Hydrocolloids, 63*, 727-734.

Thepkunya, H., Rungnaphar, P., & Mcclements, D. J. (2006). Stabilization of model beverage cloud emulsions using protein-polysaccharide electrostatic complexes formed at the oil-water interface. *Journal of Agricultural & Food Chemistry, 54*(15), 5540-5547.

Tsabet, È., & Fradette, L. (2015). Effect of the properties of oil, particles, and water on the production of Pickering emulsions. *Chemical Engineering Research & Design, 97*, 9-17.

Van, F. D. V., De, E. H., Oosterveld, A., & Tromp, R. H. (2015). Protein-polysaccharide interactions to alter texture. *Review of Food Science & Technology, 6*(1), 371-388.

Wagoner, T., Vardhanabhuti, B., & Foegeding, E. A. (2016). Designing Whey Protein–Polysaccharide Particles for Colloidal Stability. *Annual Review of Food Science & Technology, 7*(1), 93-116.

Wu, M. A., Xiong, Y. L. L., Jie, C., Tang, X. Y., & Zhou, G. H. (2009). Rheological and microstructural properties of porcine myofibrillar protein-lipid emulsion composite gels. *Journal of Food Science, 74*(4), 207-217.

Yanjun, S., Jianhang, C., Shuwen, Z., Hongjuan, L., Jing, L., Lu, L., Uluko, H., Yanling, S., Wenming, C., & Wupeng, G. (2014). Effect of power ultrasound pre-treatment on the physical and

functional properties of reconstituted milk protein concentrate. *Journal of Food Engineering, 124*(4), 11-18.

Yuan, F., Xu, D., Qi, X., Zhao, J., & Gao, Y. (2013). Impact of High Hydrostatic Pressure on the Emulsifying Properties of Whey Protein Isolate–Chitosan Mixtures. *Food & Bioprocess Technology, 6*(4), 1024-1031.

Table 1. The surface tension, d_{43} and d_{32} values, and the power-law model of the emulsions

	Surface tension	Particle size (μm)		Parameters of power-law model		
	(mN/m)	d_{43}	d_{32}	n	K	R^2
0 W	34.77 ± 0.45[a]	18.40 ± 0.36[a]	10.37 ± 0.60[f]	0.115	1.121	0.9873
150 W	29.10 ± 0.36[c]	12.83 ± 0.15[d]	6.90 ± 0.07[h]	0.171	0.751	0.9931
300 W	26.73 ± 0.21[d]	12.03 ± 0.35[e]	6.54 ± 0.13[h]	0.195	0.574	0.9945
450 W	27.13 ± 0.45[d]	14.60 ± 0.36[c]	8.09 ± 0.13[g]	0.323	0.272	0.9924
600 W	32.00 ± 0.17[b]	17.67 ± 0.65[b]	8.55 ± 0.40[g]	0.486	0.068	0.9840

Means within a column followed by a different letter are significantly different ($p < 0.05$).

Highlights

- Effects of ultrasonic treatments on MP-XG emulsion were evaluated.
- Ultrasonic treatment improved the stability of MP-XG emulsion.
- Functional groups of MP-XG remained unchanged after ultrasonic treatment.
- Ultrasonic treatment reduced the apparent viscosity of MP-XG emulsion.

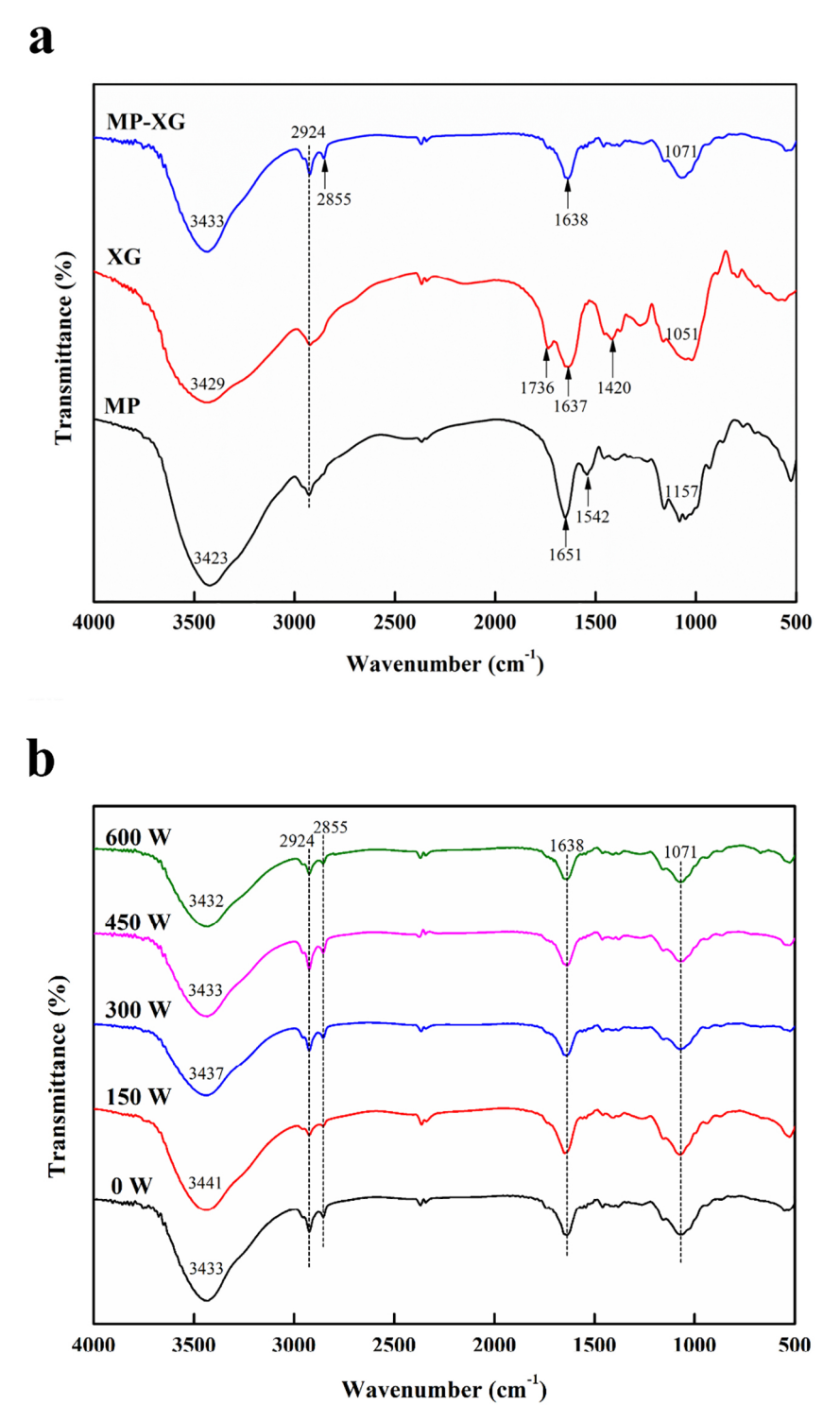
a
MP-XG
XG
MP
3433
2924
2855
1638
1071
3429
1736
1637
1420
1051
3423
1651
1542
1157
Transmittance (%)
4000
3500
3000
2500
2000
1500
1000
500
Wavenumber (cm-1)
b
600 W
450 W
300 W
150 W
0 W
3432
3433
3437
3441
3433
2924
2855
1638
1071
Transmittance (%)
4000
3500
3000
2500
2000
1500
1000
500
Wavenumber (cm-1)

Figure 1

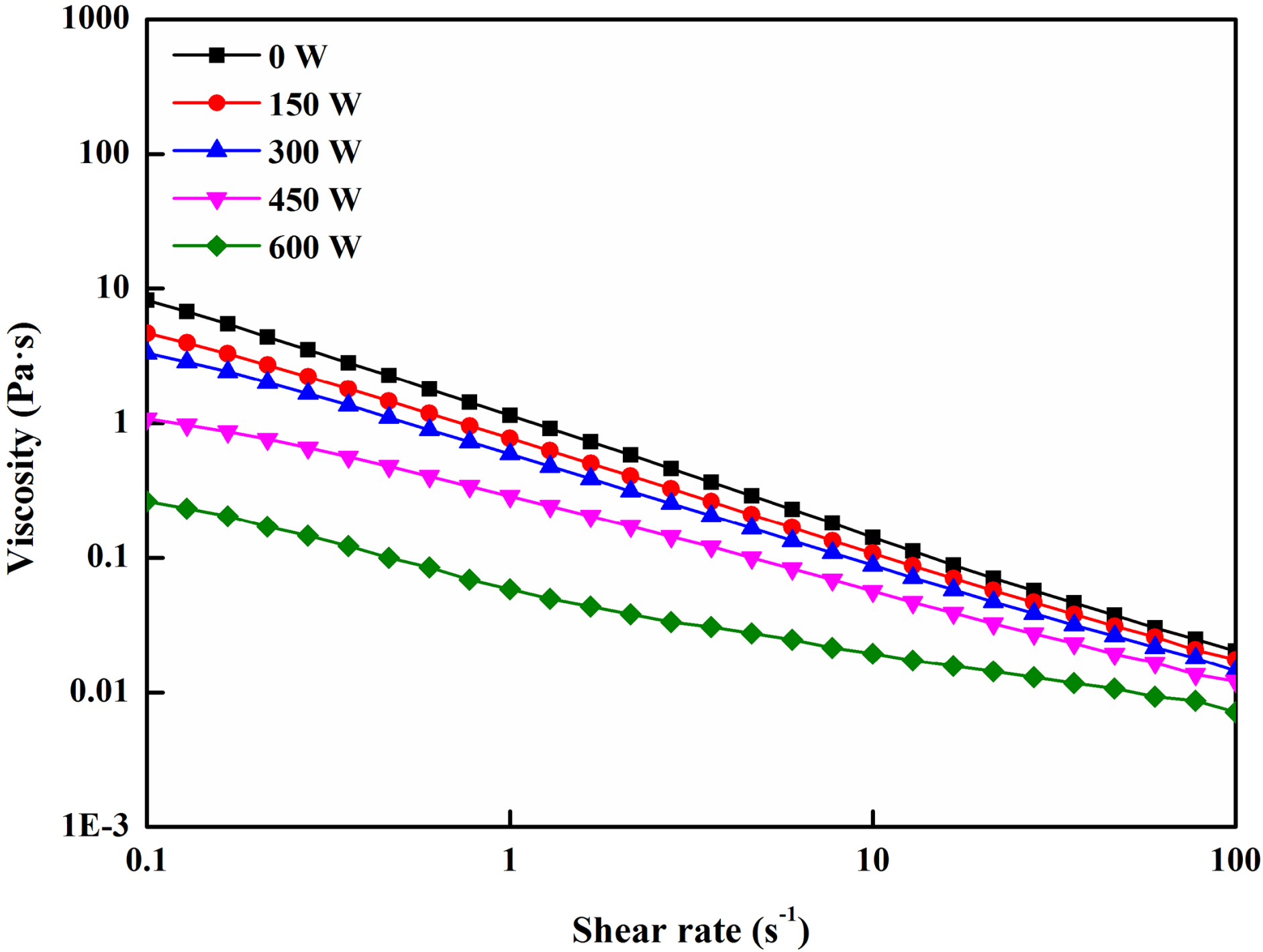
1000
100
10
1
0.1
0.01
1E-3
0.1
1
10
100
Viscosity (Pa·s)
Shear rate (s-1)
0 W
150 W
300 W
450 W
600 W

Figure 2

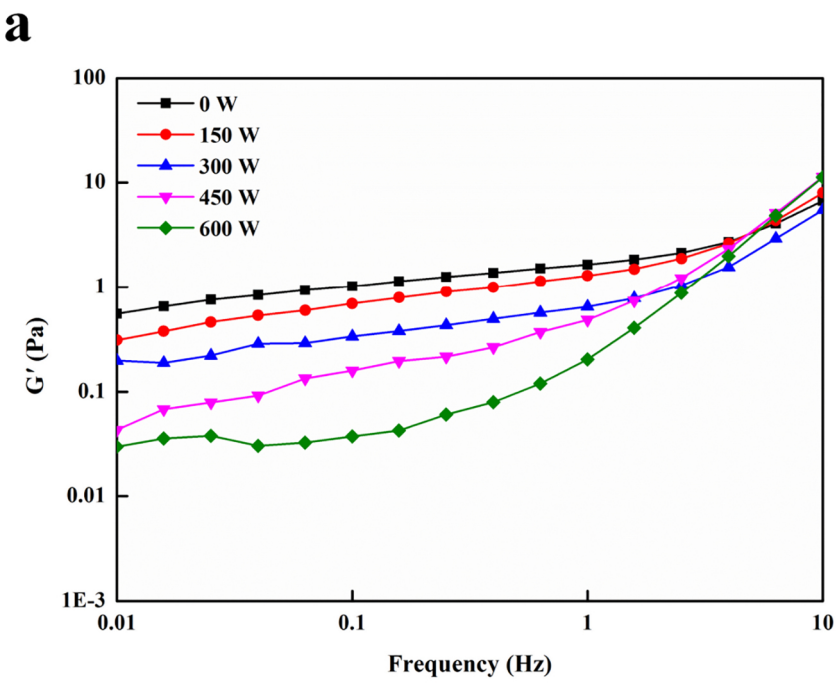
a
100
10
1
0.1
0.01
1E-3
G′ (Pa)
0 W
150 W
300 W
450 W
600 W
0.01
0.1
1
10
Frequency (Hz)

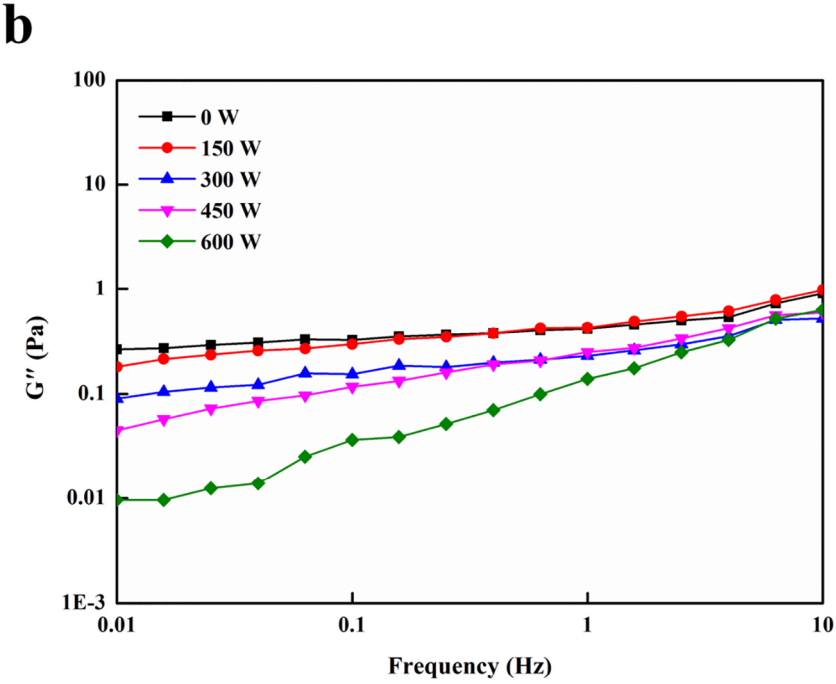
b
100
10
1
0.1
0.01
1E-3
G″ (Pa)
0 W
150 W
300 W
450 W
600 W
0.01
0.1
1
10
Frequency (Hz)

Figure 3

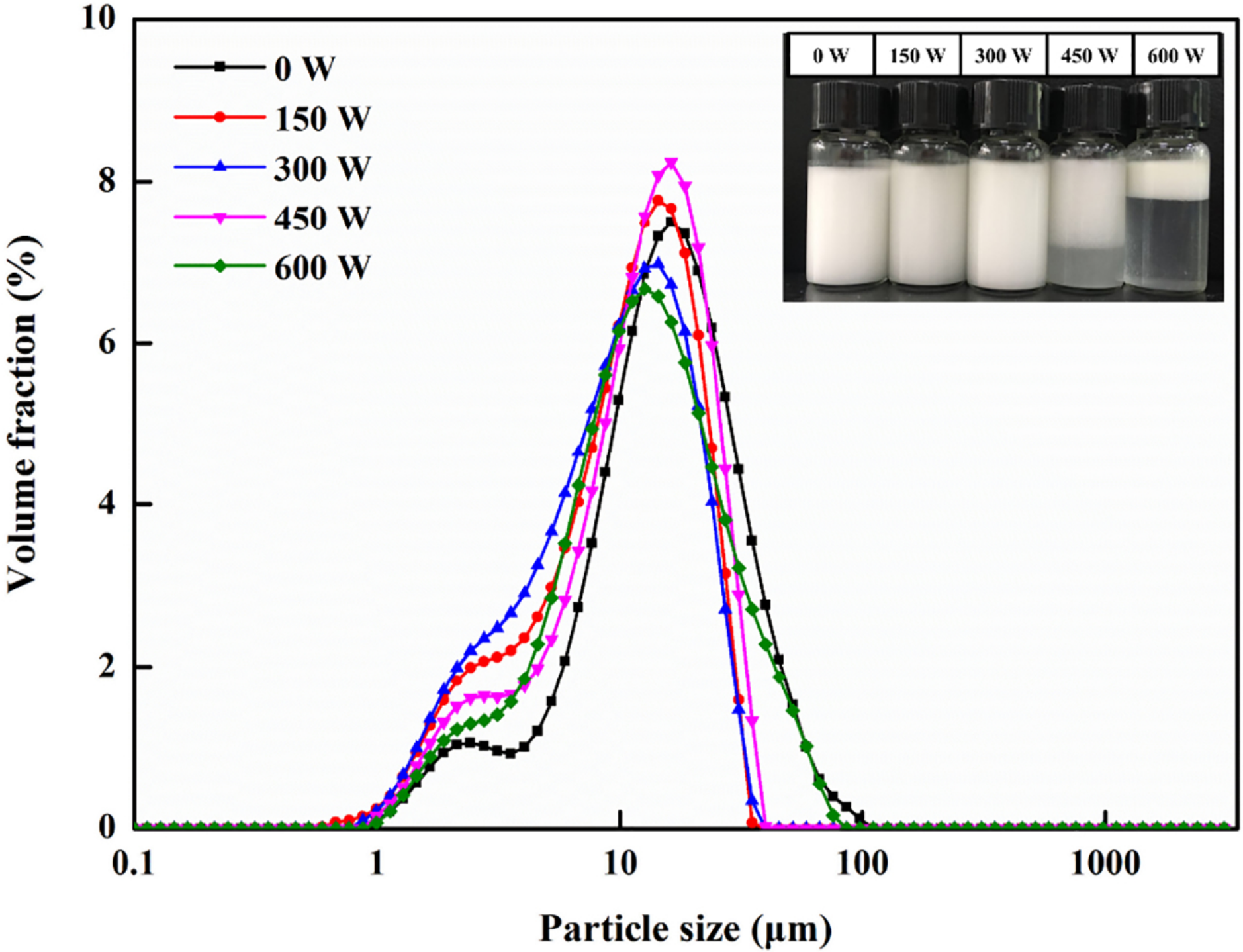
0 W
150 W
300 W
450 W
600 W
Volume fraction (%)
Particle size (μm)
0
2
4
6
8
10
0.1
1
10
100
1000
0 W
150 W
300 W
450 W
600 W

Figure 4

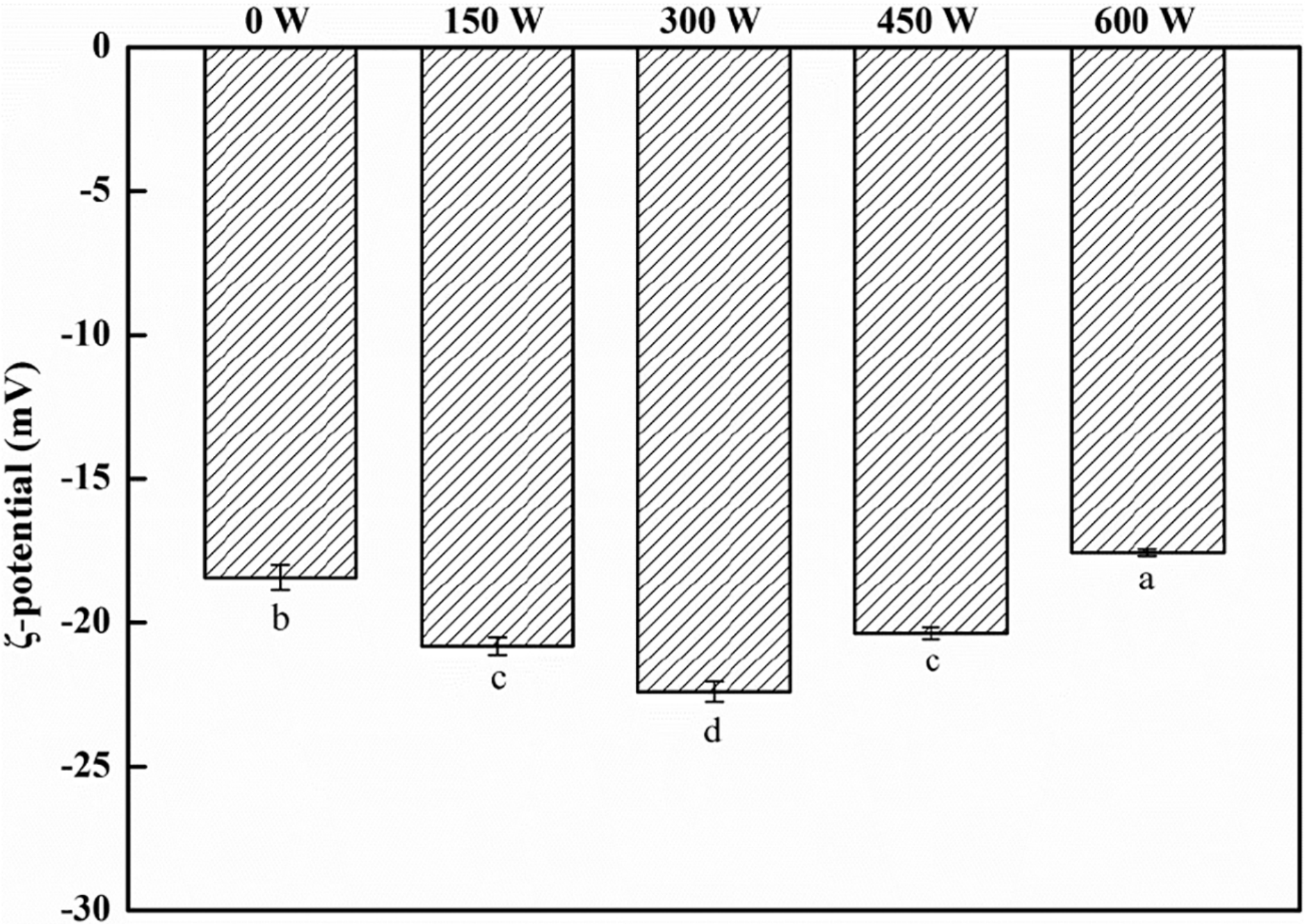

Figure 5

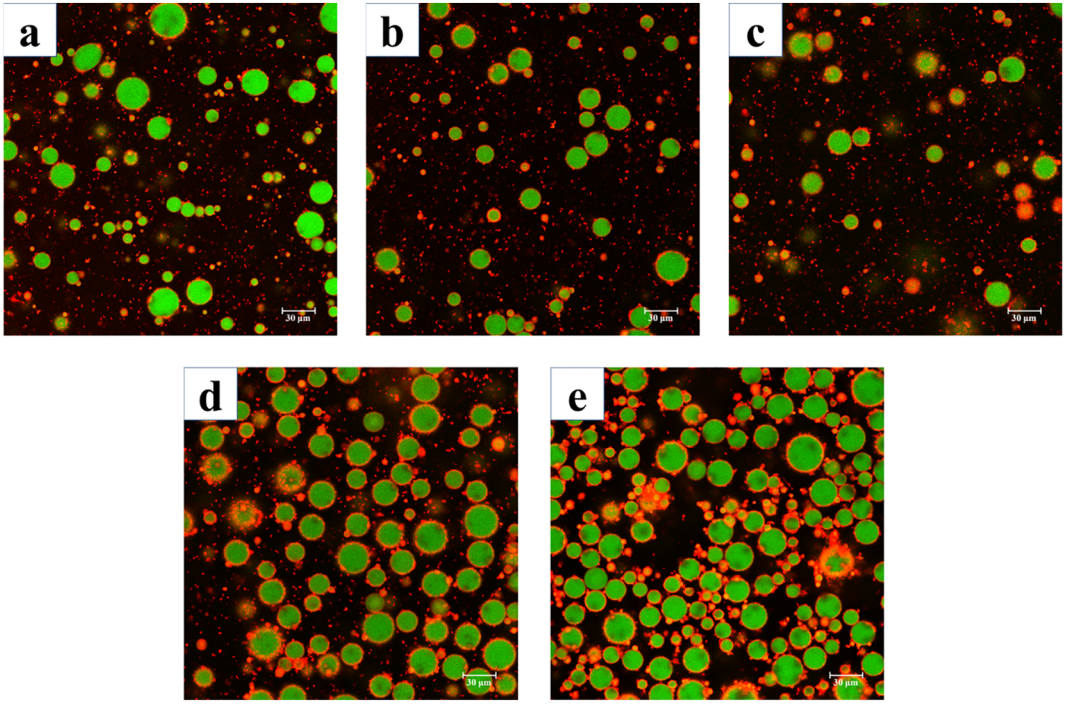

Figure 6

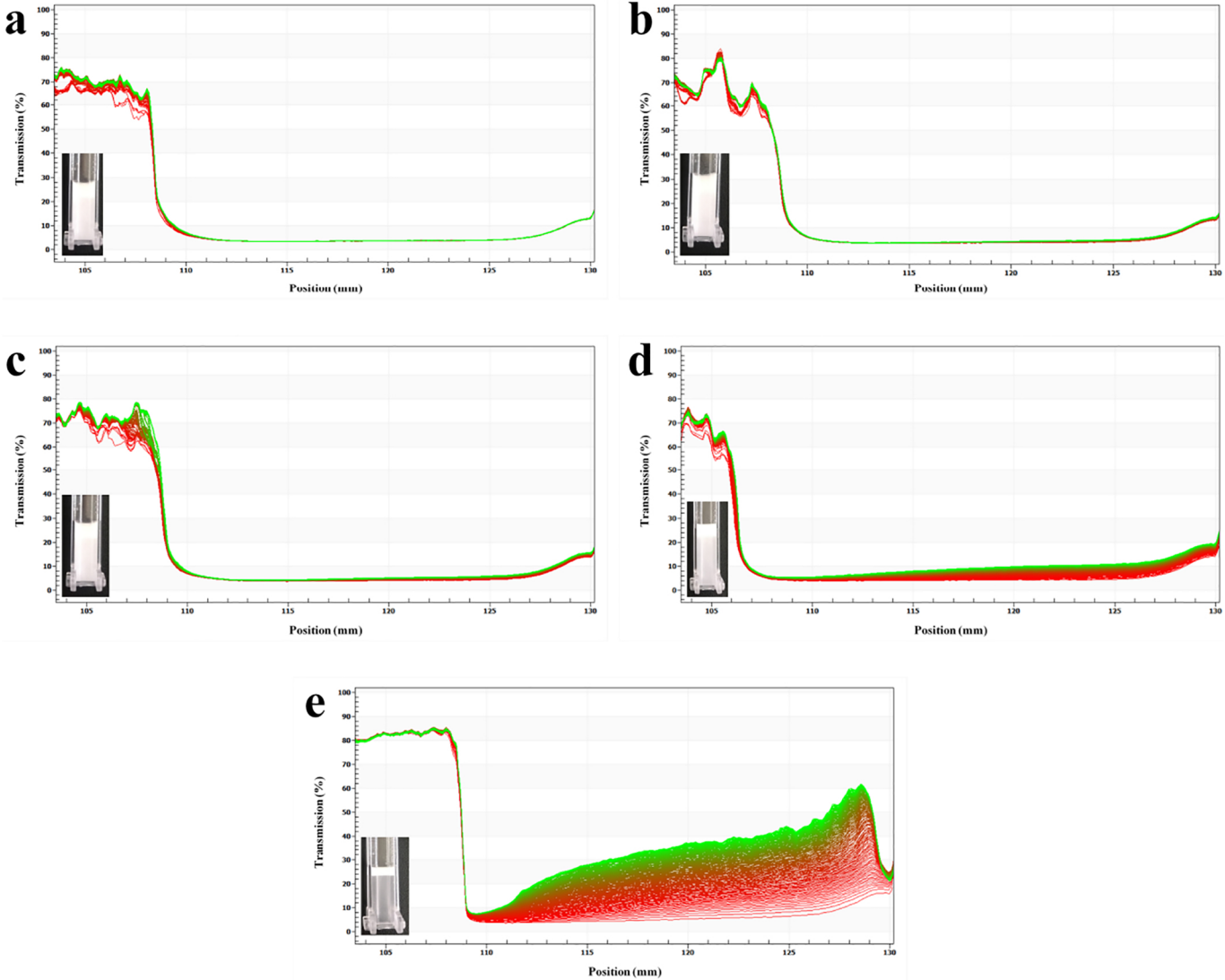

Figure 7